

Distinguishing Gasoline Engine Oils of Different Viscosities Using Terahertz Time-Domain Spectroscopy

Ali Mazin Abdul-Munaim^{1,2} · Marco Reuter³ ·
Martin Koch³ · Dennis G. Watson¹

Received: 23 February 2015 / Accepted: 22 April 2015 /
Published online: 7 May 2015
© Springer Science+Business Media New York 2015

Abstract Terahertz-time-domain spectroscopy (THz-TDS) in the range of 0.5–2.0 THz was evaluated for distinguishing among gasoline engine oils of three different grades (SAE 5W-20, 10W-40, and 20W-50) from the same manufacturer. Absorption coefficient showed limited potential and only distinguished ($p < 0.05$) the 20W-50 grade from the other two grades in the 1.7–2.0-THz range. Refractive index data demonstrated relatively flat and consistently spaced curves for the three oil grades. ANOVA results confirmed a highly significant difference ($p < 0.0001$) in refractive index among each of the three oils across the 0.5–2.0-THz range. Linear regression was applied to refractive index data at 0.25-THz intervals from 0.5 to 2.0 THz to predict kinematic viscosity. All seven linear regression models, intercepts, and refractive index coefficients were highly significant ($p < 0.0001$). All models had a similar fit with R^2 ranging from 0.9773 to 0.9827 and RMSE ranging from 6.33 to 7.75. The refractive indices at 1.25 THz produced the best fit. The refractive indices of these oil samples were promising for identification and distinction of oil grades.

Keywords Terahertz spectroscopy · Engine oil · Oil condition · Kinematic viscosity

1 Introduction

Internal combustion engines in automobiles, trucks, tractors, boats, and industrial equipment are dependent on circulating engine oil to prevent rapid engine failure. Metal-to-metal contact

✉ Dennis G. Watson
dwatson@siu.edu

¹ Department of Plant, Soil and Agricultural Systems, College of Agricultural Sciences, Southern Illinois University, Carbondale, IL 62901, USA

² Department of Agricultural Machines and Equipment, College of Agriculture, Baghdad University, Baghdad, Iraq

³ Faculty of Physics and Material Sciences Center, Philipps-Universität Marburg, Renthof 5, 35032 Marburg, Germany

points in an internal combustion engine rely on a thin film of oil for lubrication. Additives of modern engine oils also clean, inhibit corrosion, resist oxidation, neutralize acids, bind contaminants, and improve sealing [1].

Regardless of the brand or composition, engine oil has a finite life and cannot indefinitely perform its vital functions in an engine. During use, engine oil is subjected to oxidation and contaminants that reduce its effectiveness. For these reasons, engine manufacturers recommend an oil change interval at which used oil is replaced with new oil. Manufacturers provide only general recommendations for oil change intervals, which may not match an engine's use. In one case, an automobile driven long distances at highway speeds and relatively low engine speeds, the engine oil may be able to perform satisfactorily for twice as long as the manufacturer's recommended change interval. In another case of farm tractor or industrial equipment operating continuously at near full power in extremely dusty conditions, the motor oil may be "used up" in less than half the manufacturer's recommended change interval. In the first case, useful oil is discarded and unnecessary maintenance costs are incurred. In the second case, the service life of the engine is shortened due to wear and much higher costs may be incurred to renew or replace the engine.

Testing is needed to monitor the useful life of engine oil. Several companies offer oil analysis services, but customers must collect a sample of engine oil on regular intervals and send for analysis. This method has not been commonly used by consumers due to the requirement of withdrawing an oil sample and the cost of the analysis. New technology is desired that would allow in situ or at least on-site oil analysis.

Many researchers have tested sensor systems for in situ or on-site oil analysis. Sensor systems researched have included infrared [2–4], hyperspectral [5], resonating [6–10], and electrochemical [11–16]. These sensors have attempted to monitor oil conditions such as viscosity [7, 8, 12, 17]; acidity [6, 14–16, 18]; fuel, water, or antifreeze contamination [3]; and antioxidants [11, 13]. Some combination of the above sensors was preferred to meet the requirements of oil condition monitoring [9, 17].

So far, no oil condition monitoring sensor has been widely implemented in engines. Automobile manufacturers have implemented algorithms that use input from other engine sensors as a proxy for an oil condition sensor. While these algorithms may allow extended oil change intervals they may not adequately compensate for fuel differences with flex-fuel vehicles or for synthetic and conventional oil differences [19].

Terahertz (THz) spectroscopy has emerged as another technology for characterization of fluids. Many applications of THz spectroscopy have been identified [20, 21], including petroleum products. Prior research using THz-time-domain spectroscopy (THz-TDS) to distinguish among petroleum and related products includes the following: three grades of gasoline [22], gasoline and diesel fuel [23], ethanol and gasoline mixtures [24], diesel fuel grades [25], diesel fuel solidifying point [26], biodiesel and base stocks [27], gasoline and diesel fuel [28] inflammable liquids [29], lubricating grease [30], polyglycol oils with water [31], mineral oil with additives [32], six grades of lubricating oil [33], oil base stock and additive [34], and vegetable oils [35, 36]. These prior studies demonstrated potential for distinguishing petroleum products, but none evaluated the potential for distinguishing among similar gasoline engine oils of different grades/viscosities.

THz technology and spectroscopy is a rapidly developing field [20]. Although there are many schemes to generate and detect THz waves, THz-TDS [37, 38] is the most powerful and widely used technique. This technique relies on photoconductive antennas which are gated by ultrashort laser pulses [39–42]. Alternatively, nonlinear crystals can be used [43]. Using this

scheme, many substances have been characterized. This includes gases [44, 45], liquids [46], liquid crystals [47, 48], and different types of solids [49–53]. But also, artwork [54] and plants [55, 56] have been investigated by THz-TDS.

1.1 Research Objective

The objective of this study was to determine if samples from three different grades of fresh gasoline engine oil could be distinguished with THz-TDS. If successful, THz-TDS would be an alternative for further evaluation as a means of determining oil viscosity and potentially other oil characteristics.

2 Experimental

2.1 Oil Sample Preparation

Three grades of Pennzoil® gasoline motor oil in 946-mL containers were purchased from a local retailer (Carbondale, IL, USA). The grades were SAE 5W-20, 10W-40, and 20W-50 and all were rated for API service category SN. The same trade name was purchased for each grade of oil to minimize differences in the oil composition. Although the actual oil composition was proprietary, the grades were assumed to be similar, but vary with viscosity either of the base stock or through viscosity modifiers. This difference in oil composition by SAE grade or viscosity was expected to be reflected in THz-TDS spectroscopy.

A sample of each oil was prepared for kinematic viscosity measurement. Approximately 100 mL of each oil grade was placed in a plastic container. The oil samples were coded and no information was provided for identification of the oil grade. The samples were shipped to Blackstone Labs (Fort Wayne, IN, USA) for kinematic viscosity measurement according to ASTM D445 [57]. ASTM D445 specifies two temperatures for viscosity measurement, 40 and 100 °C. The 40 °C test was specified for these samples to better represent room temperature viscosity, as THz-TDS spectroscopy was conducted at room temperature.

Another set of samples were prepared by pouring approximately 100 mL of each of the three grades of oil into a separate amber, round bottle (Qorpak™ GLC-01935, Fisher Scientific, Pittsburgh, PA, USA). The samples were also coded and shipped to the Experimental Semiconductor Physics Lab at Phillips University (Marburg, Germany) for THz-TDS analysis.

2.2 THz-Time-Domain Spectrometer

A schematic of the THz time-domain spectrometer was depicted in Fig. 1. A Ti:sapphire laser was optically pumped by a frequency doubled Nd:YVO₄ laser to produce 100 fs pulses with a central wavelength of 800 nm and a repetition rate of 80 MHz. These laser pulses were used to gate the photoconductive antennas for the generation and detection of THz pulses. The antennas consisted of a semiconductor substrate and a pair of coplanar metal striplines. The laser pulses excited the semiconductor between the two striplines to generate electrons and holes. At the emitter, these carriers were excited by an applied bias. The resulting current pulse was the source for a THz pulse radiated in free-space. After passing some optical components

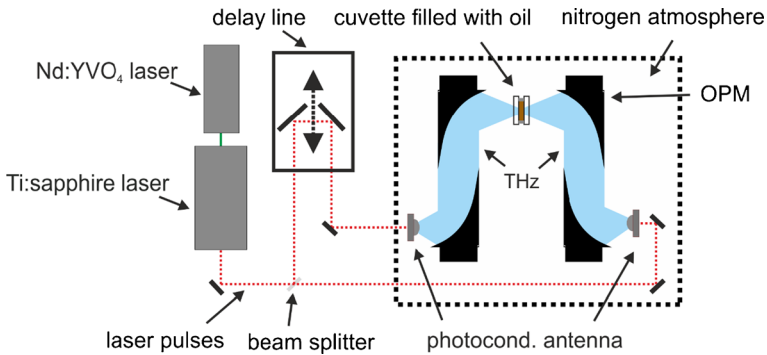


Fig. 1 Schematic of the THz time-domain spectrometer

such as silicon lenses, off-axis parabolic mirrors (OPM), and the sample, the transmitted THz pulse was focused onto the receiver antenna. In contrast to the emitter antenna, the optically excited carriers were not accelerated by an applied external field but instead by the field of the incident THz pulse. Hence, the THz field biased this antenna which gave rise to a net current which was detected by a lock-in amplifier. A THz waveform which resembles the real THz pulse was detected by varying the delay between the gating laser pulse and the incoming THz pulse (see [20] for details).

The oil samples were filled in a customized cell [47]. It consisted of two 700- μm fused silica plates, which were nearly transparent at THz frequencies. The windows were separated by two copper plates leading to a distance between the plates of 5.9 mm, which is the thickness the THz radiation needs to pass. Such thick cells were chosen to improve the interaction length due to the low absorption of the oil samples (Fig. 4).

For the data extraction of the oil samples, first, the two fused silica plates were measured separately and their material parameters were calculated taking multiple reflections into account [58]. Then, the cell was built, filled with the oil sample, and the time domain data was recorded in the THz setup. The material parameters of the oil samples were determined by using a highly accurate data extraction algorithm including the information of the windows [59].

2.3 THz-TDS Data Analysis

Data of frequency, refractive index, and absorption coefficient from each of three tests of each of the three gasoline engine oil samples were further analyzed. Mean, standard deviation, and 95 % confidence interval of refractive index and absorption coefficient were calculated for each sample at each frequency and plotted. Analysis of variance (ANOVA) was used to determine if there was a significant difference ($\alpha=0.05$) in refractive index or absorption coefficient among the oil weights at each frequency. Tukey's test was used to distinguish among oil samples when a significant difference existed.

Similar to Zhao [26], regression analysis was completed on the best potential predictor value (refraction index or absorption coefficient) using data at multiple frequencies (0.5–2.0 THz at 0.25-THz intervals). The linear models were evaluated on coefficient of determination (R^2) and root mean square error (RMSE). SAS® Enterprise Guide 6.1 software [60] was used for ANOVA, Tukey's test, and linear regression analysis.

3 Results and Discussion

3.1 Kinematic Viscosity

The results of the ASTM D445 [57] 40 °C kinematic viscosity test of the three oil grades were depicted in Fig. 2. As expected, the measured viscosity increased for the heavier grades of oil. The differences in the oil sample viscosities confirmed by the kinematic viscosity test were promising for the THz-TDS method to be able to distinguish the oils.

3.2 THz-TDS

Data from the THz time-domain spectrometer resulted in 310 frequencies ranging from about 0.5 to 2.0 THz with an increment of approximately 0.0049 THz. Refractive indices and absorption coefficients were available for further analysis.

3.2.1 Refractive Index

The refractive indices for each of the three grades of oil were illustrated in Fig. 3. The curves were relatively flat and parallel. The refractive index increased with the heavier oil grades. The refractive index difference between the 5W-20 sample mean and the 10W-40 sample mean was approximately 0.010 across the entire frequency range. Between the 10W-40 and 20W50 sample means, the difference in refractive indices was slightly less ranging from 0.0072 to 0.0078 across the THz range. There was little variation among repetitions of the same oil grade. Each oil grade exhibited a similar pattern with the confidence interval increasing

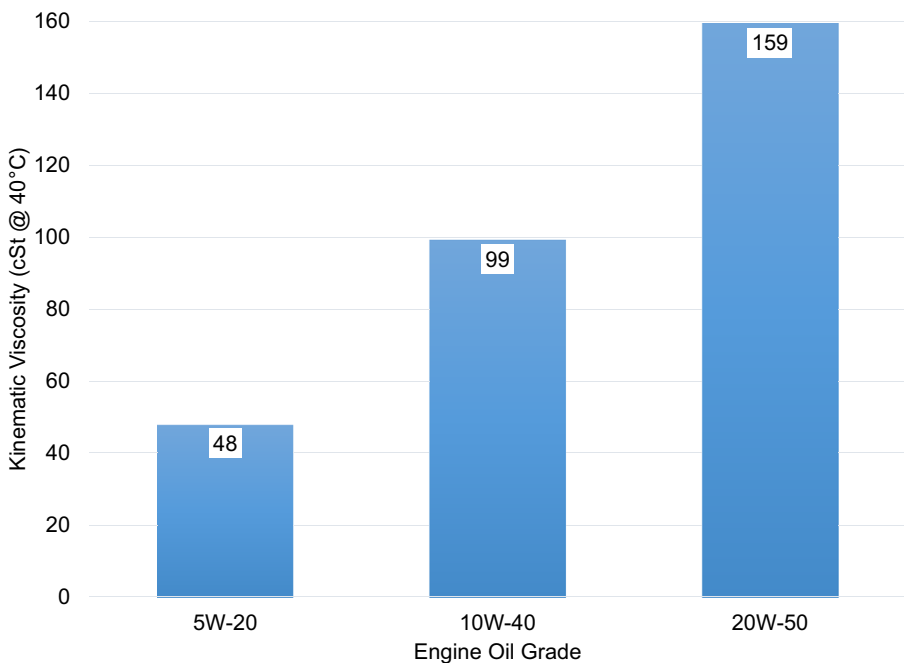


Fig. 2 Kinematic viscosity (cSt at 40 °C) for each engine oil grade based on ASTM D445

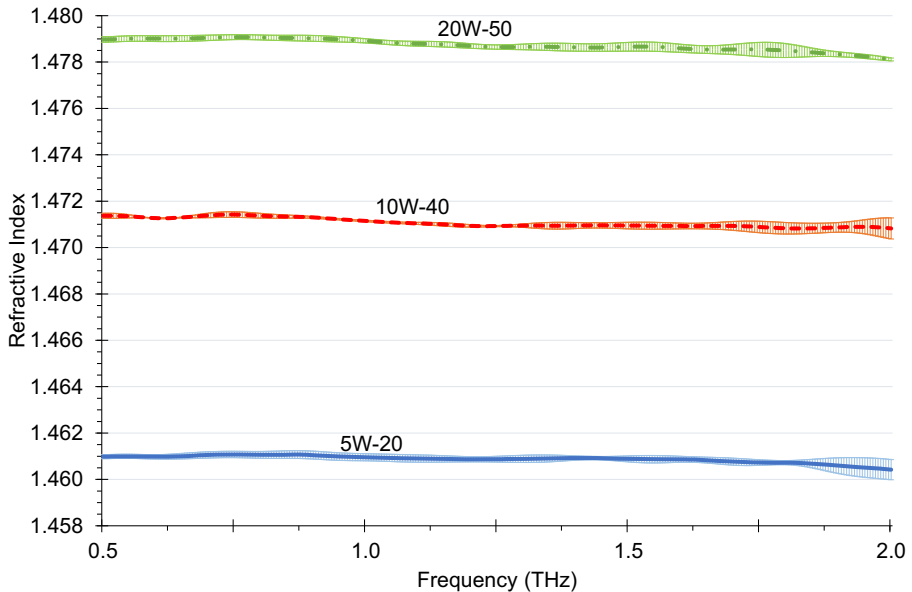


Fig. 3 Mean refractive index ($n=3$) of three fresh oil samples of different grades with 95 % confidence interval bars

slightly at the higher frequencies. The refractive indices at 1.0 THz for 5W-20, 10W-40, and 20W-50 oil grades were 1.4610, 1.4711, and 1.4789, respectively, with standard deviations of 0.00014, 0.00003, and 0.00008, respectively. Across the THz range, the standard deviation among the replications for each of the 5W-20, 10W-40, and 20W-50 oil grades peaked at 0.00090, 0.00043, and 0.00110, respectively.

These refractive index curve patterns indicate high repeatability among the same samples and distinct differences among the oil grades. ANOVA results confirmed a highly significant difference ($p < 0.0001$) among oil grades at each frequency. At each frequency, the refractive indices of each of the three oil grades was significantly different from the other two, with 5W-20 the lowest and 20W-50 the highest. The refractive indices of these oil samples were promising for identification and distinction of oil grades.

The refractive index curve patterns have varied among studies of petroleum products. The relatively flat curve patterns of refractive index in this study were similar to the patterns of gasoline and diesel fuel [23] [28], inflammable liquids [29], and lubricating grease [30]. In some studies, the refractive indices have increased with frequency. A study of diesel fuel grades had refractive indices that varied by nearly 0.07 as they increased with frequency and across the three grades, the differences in refractive index ranged from about 1.20 to 1.40 [25]. A gasoline engine oil of service category SF, but unreported grade, had a refractive index curve that increased from about 1.44 to 1.465 over the range of 0.5–1.6 THz [33].

Alternatively, refractive indices have decreased with frequency. Four vegetable oils [36] and five vegetable oils [35] had refractive indices that decreased with frequency. The refractive index of polyglycol oil decreased with frequency from about 1.55 to 1.45 across the 0.5–2.5-THz range [31]. A differing base stock and additive package in the polyglycol transmission oil may account for the declining indices with increasing frequency.

Refractive indices obtained in this study compared reasonably with other petroleum products. The indices of the oil samples at 1.0 THz of 1.461–1.479 were higher than reported gasoline indices of 1.407–1.448 [22, 23, 28, 29] and 10 % ethanol/gasoline mix of about 1.450 [24]. These differences may make it possible to identify gasoline contamination of the engine oils in this study.

The refractive indices of the 5W-20 oil at 1.0 THz of 1.461 was well above the range of three diesel fuel grades of 1.240–1.375 [25] and a single grade of diesel fuel at 1.455 [28], but overlapped with another diesel fuel measured at 1.465 [23]. This overlap could make it difficult to identify diesel fuel as a contaminant in the 5W-20 gasoline engine oil. However, diesel engines typically use a higher SAE grade, such as 15W-40 with a formulation specifically for diesel engines. The engine oil refractive indices at 1.0 THz were lower than the indices of 1.48–1.49 observed for four vegetable oils [36].

3.2.2 Absorption Coefficient

The absorption coefficients for each of the three grades of oil were illustrated in Fig. 4. The curves exhibit somewhat similar patterns with considerable overlap of the 95 % confidence interval for the samples. ANOVA indicated a significantly higher absorption coefficient of 20W-50 oil grade compared to the other two grades, in the range of 1.7–2.0 THz. Compared to refractive index, oil grade had a lesser effect on THz absorption [32]. Use of absorption coefficient to uniquely distinguish these grades of motor oil would be difficult, with the exception of the 20W-50 grade within the 1.7–2.0-THz range.

The overall pattern of increasing absorption coefficient with increasing frequency was similar to patterns of transmission fluid [31], inflammable liquids [29], petroleum fuels and substitutes [28], diesel fuel grades [25], gasoline engine oil of SF service category [33],

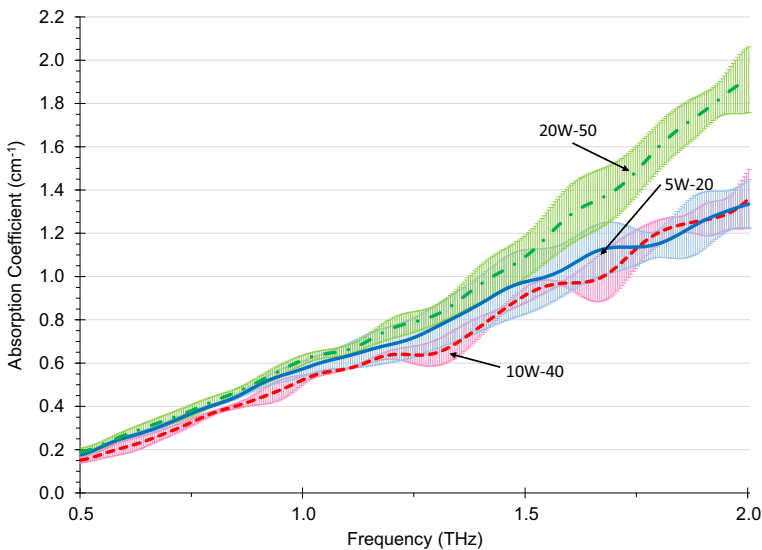


Fig. 4 Mean absorption coefficient ($n=3$) of three fresh oil samples of different grades with 95 % confidence interval bars

lubricating grease [30], vegetable oils [35, 36], grades of gasoline [22], diesel and gasoline [23], and ethanol and gasoline blends [24].

3.3 Refractive Index as Predictor of Viscosity

Based on the refractive indices (Fig 3) and absorption coefficients (Fig 4), the refractive index was of most interest for predicting viscosity. Data from seven frequencies (0.5–2.0 THz at 0.25-THz intervals) were used for linear regression analysis. All seven models were highly significant ($p < 0.0001$) and both the intercept and refractive index coefficient were highly significant ($p < 0.0001$). All models had a similar fit with R^2 ranging from 0.9773 to 0.9827 and RMSE ranging from 6.33 to 7.75. The relatively consistent differences in refractive indices across the 0.5–2.0-THz range for the three oil grades/viscosities and the increased refractive index as oil kinetic viscosity increased (Fig 3) resulted in a strong positive linear relationship. The refractive indices at 1.25 THz (Fig. 5) produced the best fit with the highest $R^2 = 0.9827$ and lowest RMSE of 6.33. The resulting linear equation was as follows:

$$\text{Kinematic viscosity} = -8995.53 + 6188.15(\text{refractive index}) \quad (1)$$

Based on oil samples in this study, THz-TDS analysis demonstrated potential for distinguishing among oil grades. THz-TDS should be considered for further evaluation as a means of determining oil viscosity and potentially other oil characteristics. Although not measured in this study, GHz frequencies may also have potential for distinguishing among oil grades if the relatively consistent refractive indices continue at GHz frequencies.

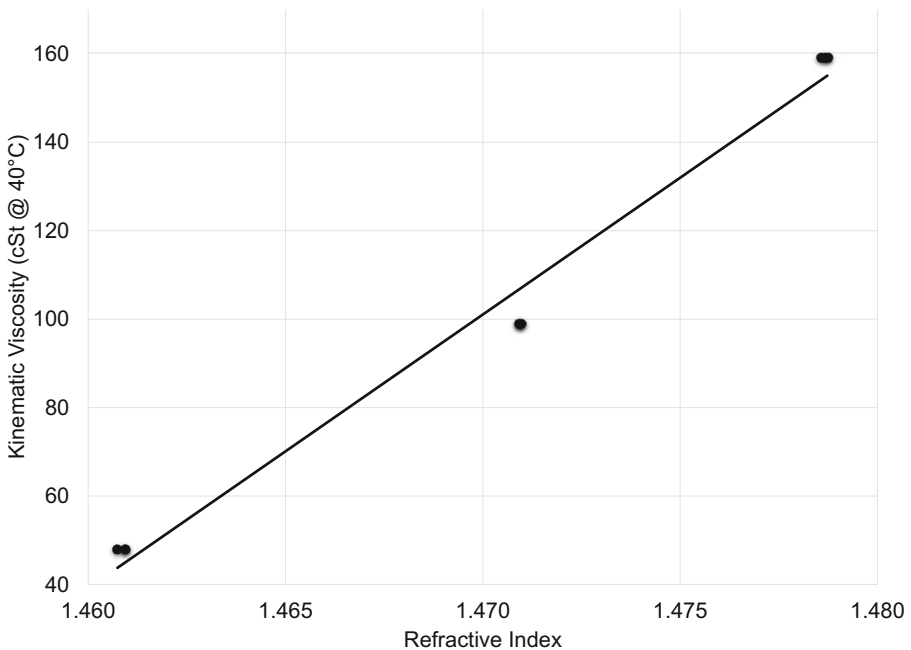


Fig. 5 Actual refractive indices (round markers) ($n=9$) and predicted kinematic viscosity at 40 °C (trend line) based on linear regression of refractive indices at 1.25 THz ($R^2=0.9827$, RMSE=6.63)

4 Conclusions

Three engine oil samples of different grades (SAE 5W-20, 10W-40, and 20W-50) were examined with THz-TDS to determine if they could be distinguished. The refractive indices were strong indicators of oil grade and viscosity. The refractive index increased with the oil viscosity. The refractive index curves of the three oil samples were relatively flat, with a consistent separation distance of 0.007–0.010 across the range of 0.5–2.0 THz. ANOVA results indicated a highly significant difference ($p < 0.0001$) among oil grades at each frequency. At each frequency, the refractive indices of each of the three oil grades was significantly different from the other two.

Absorption coefficient provided some potential for distinguishing oil samples. In the range of 1.7–2.1 THz, the 20W-50 oil sample could be distinguished from the other two grades.

A highly significant regression equation ($p < 0.0001$, $R^2 = 0.9827$, RMSE = 6.63) was determined to estimate kinematic viscosity based on refraction index at 1.25 THz. Other frequencies resulted in similar regression lines.

The refractive indices of these oil samples were promising for identification and distinction of oil grades. Future work should be conducted to verify the use of refractive indices to distinguish a wider selection of engine oil. Additionally, the use of THz-TDS should be evaluated for distinguishing contaminants in engine oil.

Acknowledgments The University of Baghdad, Baghdad, Iraq, provided partial support of this project through a Ph.D. student scholarship. The contribution of the Experimental Semiconductor Physics Lab researchers at Phillips University (Marburg, Germany) in conducting the THz-TDS analysis was greatly appreciated.

Conflict of Interest The authors declare that they have no conflict of interest.

References

1. D. Mackney, N. Clague, G. Brown, G. Fish, J. Durham, in *Automotive Lubricants and Testing*, ed. By S. C. Tung, G. E. Totten (ASTM, West Conshohocken, PA, 2012), p. 23
2. M. Blanco, J. Coello, H. Iturriaga, S. Maspoch, R. Gonzalez, *Mikrochim. Acta* (1998) doi:10.1007/BF01243055
3. A. Borin, R. J. Poppi, *Vib. Spectrosc.* (2005) doi:10.1016/j.vibspec.2004.05.003
4. J. Kasberger, T. Fromherz, A. Saeed, B. Jakoby, *Vib. Spectrosc.* (2011) doi:10.1016/j.vibspec.2011.01.003
5. H.-B. Liu, X.-C. Zhang, Y. Hu, X.-H. Wang, L.-T. Guo, C.-L. Zhang, *Acta Phys. Sin.* 54, 4124 (2005)
6. A. Agoston, C. Otsch, B. Jakoby, *Sensors Actuat. A-Phys.* (2005) doi:10.1016/j.sna.2005.02.024
7. R. J. Clark, C. M. Fajardo, *Tribol. T.* (2012) doi:10.1080/10402004.2012.670892
8. B. Jakoby, M. Scherer, M. Bushkies, H. Eisenschmid, *IEEE Sens. J.* (2003) doi:10.1109/JSEN.2003.817164
9. J. Milpied, M. Urrich, B. Patissier, L. Bernasconi, *SAE Int. J. Fuels Lubr.* (2010) doi:10.4271/2009-01-2639
10. A. J. Mohammed, M. A. M. Hassan, *Sci. Technol.* (2013) doi:10.5923/j.scit.20130301.05
11. G. T. Cheek, R. Mowery, *Anal. Chem.* (1989). doi:10.1021/ac00188a034
12. J. K. Duchowski, H. Mannebach, *Tribol. Trans.* (2006) doi:10.1080/10402000600885183
13. R. J. Price, L. J. Clarke, *Analyst* (1991) doi:10.1039/AN9911601121
14. M. Soleimani, M. Sophocleous, M. Glanc, J. Atkinson, L. Wang, R. J. Wood, R. I. Taylor, *Tribol. Int.* (2013) doi:10.1016/j.triboint.2013.02.030
15. S. S. Wang, H.-S. Lee, D. J. Smolenski, *Sensors Actuat. B-Chem.* (1994) doi:10.1016/0925-4005(93)00867-X
16. S. S. Wang, *Sensors Actuat. B-Chem.* (2002) doi:10.1016/S0925-4005(02)00155-7
17. J. Schmitgal, S. Moyer, *SAE Technical Pap.* (2005) doi:10.4271/2005-01-1810
18. S.-I. Moon, K.-K. Paek, Y.-H. Lee, J.-K. Kim, S.-W. Kim, B.-K. Ju, *Electrochem. Solid-State Lett.* (2006) doi:10.1149/1.2209433
19. D. Lamon, Z. Daming, *SAE Technical Pap.* (2013) doi:10.4271/2013-01-2607
20. P. U. Jepsen, D. G. Cooke, M. Koch, *Laser Photon. Rev.* (2011) doi:10.1002/lpor.201000011

21. S. K. Mathanker, P. R. Weckler, N. Wang, *Trans. ASABE* (2013) doi:[10.13031/trans.56.9390](https://doi.org/10.13031/trans.56.9390)
22. F. M. Al-Douseri, Y. Chen, X.-C. Zhang, *Int. J. Infrared Millim*, (2006) doi:[10.1007/s10762-006-9102-y](https://doi.org/10.1007/s10762-006-9102-y)
23. E. Arik, H. Altan, O. Esenturk, *J. Infrared Millimeter Terahertz Waves* (2014) doi:[10.1007/s10762-014-0081-0](https://doi.org/10.1007/s10762-014-0081-0)
24. E. Arik, H. Altan, O. Esenturk, *J. Phys. Chem. A* (2014) doi:[10.1021/jp500760t](https://doi.org/10.1021/jp500760t)
25. H. Zhao, K. Zhao, L. Tian, S. Zhao, Q. Zhou, Y. Shi, D. Zhao, C. Zhang, *Sci. China Ser. G* (2012) doi:[10.1007/s11433-011-4597-1](https://doi.org/10.1007/s11433-011-4597-1)
26. H. Zhao, K. Zhao, R. Bao, *ISRN Spectrosc.* (2012) doi:[10.5402/2012/876718](https://doi.org/10.5402/2012/876718)
27. H. Zhao, K. Zhao, L. Tian, Q. Miao, H. Ni, *Front. Optoelectron.* (2012) doi:[10.1007/s12200-012-0227-4](https://doi.org/10.1007/s12200-012-0227-4)
28. Y.-S. Jin, G.-J. Kim, C.-H. Shon, S.-G. Jeon, J.-I. Kim, *J. Korean Phys. Soc.* (2008) doi:[10.3938/jkps.53.1879](https://doi.org/10.3938/jkps.53.1879)
29. T. Ikeda, A. Matsushita, M. Tatsuno, Y. Minami, M. Yamaguchi, K. Yamamoto, M. Tani, M. Hangyo, *Appl. Phys. Lett.* (2005) doi:[10.1063/1.1999847](https://doi.org/10.1063/1.1999847)
30. L. Tian, Q.-L. Zhou, K. Zhao, Y.-L. Shi, D.-M. Zhao, S.-Q. Zhao, H. Zhao, R.-M. Bao, S.-M. Zhu, Q. Miao, C.-L. Zhang, *Chinese Phys. B.* (2011) doi:[10.1088/1674-1056/20/1/010703](https://doi.org/10.1088/1674-1056/20/1/010703)
31. S. Gorenflo, U. Tauer, I. Hinkov, A. Lambrecht, R. Buchner, H. Helm, *Chem. Phys. Lett.* (2006) doi:[10.1016/j.cplett.2006.01.108](https://doi.org/10.1016/j.cplett.2006.01.108)
32. M. Naftaly, A. P. Foulds, R. E. Miles, A. G. Davies, *Int. J. Infrared Millim.* (2005) doi:[10.1007/s10762-004-2033-6](https://doi.org/10.1007/s10762-004-2033-6)
33. L. Tian, Q. Zhou, B. Jin, K. Zhao, S. Zhao, Y. Shi, C. Zhang, *Sci. China Ser. G* (2009) doi:[10.1007/s11433-009-0310-z](https://doi.org/10.1007/s11433-009-0310-z)
34. L. Tian, K. Zhao, Q.-L. Zhou, Y.-L. Shi, C.-L. Zhang, *Chinese Phys. Lett.* (2012) doi:[10.1088/0256-307X/29/4/043901](https://doi.org/10.1088/0256-307X/29/4/043901)
35. Y. Hu, L. Guo, X. Wang, X. C. Zhang, in *Proceedings of SPIE 5640, Infrared Components and Their Applications* (2005) doi:[10.1117/12.580922](https://doi.org/10.1117/12.580922)
36. L. Jiusheng, *Appl. Spectrosc.* (2010) doi:[10.1366/000370210790619663](https://doi.org/10.1366/000370210790619663)
37. N. Vieweg, F. Rettich, A. Deninger, H. Roehle, R. Dietz, T. Gobel, M. Schell, *J Infrared Millim Terahertz Waves* (2014) doi:[10.1007/s10762-014-0085-9](https://doi.org/10.1007/s10762-014-0085-9)
38. W. Withayachummankul, M. Naftaly, *J Infrared Millim Terahertz Waves* (2014) doi:[10.1007/s10762-013-0042-z](https://doi.org/10.1007/s10762-013-0042-z)
39. M. Tani, S. Matsuura, K. Sakai, S.-i. Nakashima, *Appl. Opt.* (1997) doi:[10.1364/AO.36.007853](https://doi.org/10.1364/AO.36.007853)
40. P. U. Jepsen, R. H. Jacobsen, S. R. Keiding, *J. Opt. Soc. Am. B* (1996) doi:[10.1364/JOSAB.13.002424](https://doi.org/10.1364/JOSAB.13.002424)
41. S. Hunsche, D. M. Mittleman, M. Koch, M. C. Nuss, "New Dimensions in T-Ray Imaging," *IEICE Trans. Electron.* 81, 269 (1998)
42. E. Moreno, M. F. Pantoja, F. G. Ruiz, J. B. Roldan, S. G. Garcia, *J Infrared Millim Terahertz Waves* (2014) doi:[10.1007/s10762-014-0060-5](https://doi.org/10.1007/s10762-014-0060-5)
43. C. Winnewisser, P. U. Jepsen, M. Schall, V. Schyja, H. Helm, *Appl. Phys. Lett.* (1997) doi:[10.1063/1.119093](https://doi.org/10.1063/1.119093)
44. D. M. Mittleman, R. H. Jacobsen, R. Neelamani, R. G. Baraniuk, M. C. Nuss, *Appl. Phys. B Lasers Opt.* (1998) doi:[10.1007/s003400050520](https://doi.org/10.1007/s003400050520)
45. H. Harde, N. Katzenellenbogen, D. Grischkowsky, *Phys. Rev. Lett.* (1995) doi:[10.1103/PhysRevLett.74.1307](https://doi.org/10.1103/PhysRevLett.74.1307)
46. T. Wang, P. Klarskov, P. U. Jepsen, *IEEE Trans. Terahertz Sci. Technol.* (2014) doi:[10.1109/TTHZ.2014.2322757](https://doi.org/10.1109/TTHZ.2014.2322757)
47. N. Vieweg, C. Jansen, M. K. Shakhf, M. Scheller, N. Krumbholz, R. Wilk, M. Mikulics, M. Koch, *Opt. Express* (2010) doi:[10.1364/OE.18.006097](https://doi.org/10.1364/OE.18.006097)
48. M. Reuter, N. Vieweg, B. M. Fischer, M. Mikulicz, M. Koch, K. Garbat, R. Dabrowski, *APL Mater.* (2013) doi:[10.1063/1.4808244](https://doi.org/10.1063/1.4808244)
49. D. V. Nickel, A. J. Garza, G. Scuseria, D. M. Mittleman, *Chem. Phys. Lett.* (2014) doi:[10.1016/j.cplett.2013.12.055](https://doi.org/10.1016/j.cplett.2013.12.055)
50. S. Wietzke, C. Jansen, M. Reuter, T. Jung, D. Kraft, S. Chatterjee, B. M. Fischer, M. Koch, *J. Mol. Struct.* (2011) doi:[10.1016/j.molstruc.2011.07.036](https://doi.org/10.1016/j.molstruc.2011.07.036)
51. J. Lloyd-Hughes, T. Richards, H. Siringhaus, E. Castro-Camus, L. M. Herz, M. B. Johnston, *Appl. Phys. Lett.* (2006) doi:[10.1063/1.2340057](https://doi.org/10.1063/1.2340057)
52. O. V. Misochko, M. Tani, K. Sakai, K. Kisoda, S. Nakashima, V. N. Andreev, F. A. Chudnovsky, *Phys. Rev. B* (1998) doi:[10.1103/PhysRevB.58.12789](https://doi.org/10.1103/PhysRevB.58.12789)
53. L. Jiang, M. Li, C. Li, H. Sun, L. Xu, B. Jin, Y. Liu, *J Infrared Millim Terahertz Waves* (2014) doi:[10.1007/s10762-014-0092-x](https://doi.org/10.1007/s10762-014-0092-x)
54. J. B. Jackson, J. Bowen, G. Walker, J. Labaune, G. Mourou, M. Menu, K. Fukunaga, *IEEE Trans. Terahertz Sci. Technol.* (2011) doi:[10.1109/TTHZ.2011.2159538](https://doi.org/10.1109/TTHZ.2011.2159538)
55. E. Castro-Camus, M. Palomar, A. A. Covarrubias, *Sci. Rep.* (2013) doi:[10.1038/srep02910](https://doi.org/10.1038/srep02910)
56. N. Born, D. Behringer, S. Liepelt, S. Beyer, M. Schwerdtfeger, B. Ziegenhagen, M. Koch, *Plant Physiol.* (2014) doi:[10.1104/pp.113.233601](https://doi.org/10.1104/pp.113.233601)
57. ASTM, Standard Test Method for Kinematic Viscosity of Transparent and Opaque Liquids (and Calculation of Dynamic Viscosity) (ASTM, West Conshohocken, PA, 2014)
58. M. Scheller, C. Jansen, M. Koch, *Opt. Commun.* (2009) doi:[10.1016/j.optcom.2008.12.061](https://doi.org/10.1016/j.optcom.2008.12.061)
59. R. Wilk, I. Pupezza, R. Cemat, M. Koch, "Highly Accurate THz Time-Domain Spectroscopy of Multilayer Structures," *IEEE J. Sel. Top. Quantum Electron.* (2008) doi:[10.1109/JSTQE.2007.910981](https://doi.org/10.1109/JSTQE.2007.910981)
60. SAS Institute Inc, *SAS Enterprise Guide* (SAS Institute Inc, Cary, NC, 2013)